

## Article

## Singular Temperatures Connected to Charge Transport Mechanism Transitions in Perylene Bisimides from Steady-State Photocurrent Measurements

Jose A. Quintana, Jose M. Villalvilla, Alejandro de la Peña, José Luis Segura, and María A. Díaz-García

*J. Phys. Chem. C*, **Just Accepted Manuscript** • DOI: 10.1021/acs.jpcc.5b03152 • Publication Date (Web): 29 May 2015

Downloaded from <http://pubs.acs.org> on June 2, 2015

### Just Accepted

“Just Accepted” manuscripts have been peer-reviewed and accepted for publication. They are posted online prior to technical editing, formatting for publication and author proofing. The American Chemical Society provides “Just Accepted” as a free service to the research community to expedite the dissemination of scientific material as soon as possible after acceptance. “Just Accepted” manuscripts appear in full in PDF format accompanied by an HTML abstract. “Just Accepted” manuscripts have been fully peer reviewed, but should not be considered the official version of record. They are accessible to all readers and citable by the Digital Object Identifier (DOI®). “Just Accepted” is an optional service offered to authors. Therefore, the “Just Accepted” Web site may not include all articles that will be published in the journal. After a manuscript is technically edited and formatted, it will be removed from the “Just Accepted” Web site and published as an ASAP article. Note that technical editing may introduce minor changes to the manuscript text and/or graphics which could affect content, and all legal disclaimers and ethical guidelines that apply to the journal pertain. ACS cannot be held responsible for errors or consequences arising from the use of information contained in these “Just Accepted” manuscripts.



ACS Publications  
High quality. High impact.

1  
2  
3  
4  
5  
6  
7  
8  
9  
10  
11  
12  
13  
14  
15  
16  
17  
18  
19  
20  
21  
22  
23  
24  
25  
26  
27  
28  
29  
30  
31  
32  
33  
34  
35  
36  
37  
38  
39  
40  
41  
42  
43  
44  
45  
46  
47  
48  
49  
50  
51  
52  
53  
54  
55  
56  
57  
58  
59  
60

# Singular Temperatures Connected to Charge Transport Mechanism Transitions in Perylene Bisimides from Steady-State Photocurrent Measurements

*José A. Quintana,<sup>a</sup> José M. Villalvilla,<sup>b</sup> Alejandro de la Peña,<sup>c</sup> José L. Segura,<sup>c</sup> and María A. Díaz-García<sup>\*, b</sup>*

<sup>a</sup> Dpto. Óptica, Instituto Universitario de Materiales de Alicante y Unidad Asociada UA-CSIC, Universidad de Alicante, 03080 Alicante, Spain.

<sup>b</sup> Dpto. Física Aplicada, Instituto Universitario de Materiales de Alicante y Unidad Asociada UA-CSIC, Universidad de Alicante, 03080 Alicante, Spain.

<sup>c</sup> Dpto. Química Orgánica, Facultad de Química, Universidad Complutense de Madrid, 28040 Madrid, Spain.

1  
2  
3 ABSTRACT  
4  
5

6 Perylene bisimides (PBIs) are n-type semiconducting and photogenerating materials widely used  
7 in a variety of optoelectronic devices. Particularly interesting are PBIs that are simultaneously  
8 water-soluble and liquid-crystalline (PBI-W+LC), and thus attractive for the development of  
9 high-performing easy-processable applications in biology and “green” organic electronics. In this  
10 work, singular temperatures connected to charge transport mechanism transitions in a PBI-  
11 W+LC derivative are determined with high accuracy by means of temperature-dependent  
12 photocurrent studies. These singular temperatures include not only the ones observed at 60 °C  
13 and 110 °C, corresponding to phase transition temperatures from crystalline to liquid crystalline  
14 (LC) and from LC to the isotropic phase respectively, as confirmed by differential scanning  
15 calorimetry (DSC), but also a transition at 45 °C, not observed by DSC. By analyzing the  
16 photocurrent dependence simultaneously on temperature and on light intensity, this transition is  
17 interpreted as a change from monomolecular to bimolecular recombination. These results might  
18 be useful for other semiconducting photogenerating materials, not necessarily PBIs or even  
19 organic semiconductors, which also show transport behavior changes at singular temperatures  
20 not connected with structural or phase transitions.  
21  
22  
23  
24  
25  
26  
27  
28  
29  
30  
31  
32  
33  
34  
35  
36  
37  
38  
39  
40  
41  
42

43 KEYWORDS: charge transport, photogeneration, perylene bisimides, photocurrent,  
44 recombination  
45  
46  
47  
48  
49  
50  
51  
52  
53  
54  
55  
56  
57  
58  
59  
60

1  
2  
3 INTRODUCTION  
4

5 Among organic n-type semiconducting materials, some perylene bisimides (PBIs) present high  
6 electron affinity, and good chemical, photophysical and thermal stabilities. Thus, they have been  
7 used in the fabrication of many electronic and photonic devices, such as thin film transistors,  
8 solar cells, light emitting diodes and photodiodes.<sup>1,2</sup> In the last decade, some liquid crystalline  
9 (LC) PBIs with improved charge transport performance have been synthesized.<sup>3-5</sup> Recently, great  
10 efforts have also been dedicated to the production of water-soluble PBIs to be applied in the field  
11 of biology and pointing towards the possibility of their solution processing into “green” organic  
12 electronics using water as a nontoxic solvent.<sup>6-8</sup> A PBI that is simultaneously LC and water-  
13 soluble is the N,N'-Bis[1-(2,5,8,11-tetraoxadodec-1-yl)-3,6,9,12-tetraoxatridec-1-yl]-perylene-  
14 3,4,9,10-bis(dicarboximide) (PBI-W+LC, Figure 1). Recently, we have studied the temperature  
15 dependence of the time-of-flight charge mobility of this compound (denoted in that work as PBI-  
16 W).<sup>9</sup> From spectral studies, it was concluded that majority charge carriers are electrons. It was  
17 also found that the mobility follows an Arrhenius-type behavior up to its LC phase transition  
18 temperature, where it increases abruptly by one order of magnitude and becomes nearly  
19 temperature independent.

20 In the present study it is shown that the performance of steady-state photocurrent  
21 measurements allows determining with great accuracy singular temperatures at which changes in  
22 the dominating transport mechanism occur. In fact, this technique has been previously used by  
23 some of us to determine the glass transition temperature and other critical temperatures in  
24 photorefractive polymer composites.<sup>10,11</sup> When these temperatures are related with structural or  
25 phase transitions, they can be easily identified by differential scanning calorimetry (DSC).  
26 However, when they are not, an alternative technique involving an electrical parameter is  
27  
28  
29  
30  
31  
32  
33  
34  
35  
36  
37  
38  
39  
40  
41  
42  
43  
44  
45  
46  
47  
48  
49  
50  
51  
52  
53  
54  
55  
56  
57  
58  
59  
60

1  
2  
3 needed. In the case of PBI-W+LC, no singular temperatures, other than the ones related with  
4  
5 phase transitions, could be detected from temperature dependent mobility studies.<sup>9</sup> Here it is  
6  
7 shown that the steady-state photocurrent constitutes a very convenient parameter for such  
8  
9 purpose. It is able to determine with accuracy temperatures undetectable by neither DSC, nor  
10  
11 mobility. Moreover, it is demonstrated that the performance of temperature dependent  
12  
13 photocurrent studies in combination with the analysis of the light-intensity dependence allows  
14  
15 getting insights into the transport mechanisms taking place in PDI-W+LC, particularly the  
16  
17 charge recombination processes arising in each temperature regime. Since recombination leads to  
18  
19 a loss of photogenerated charge carriers, the identification of these processes is very useful for  
20  
21 improving the performance of modern organic electronic devices.<sup>12,13</sup> The photocurrent and other  
22  
23 derived magnitudes, such as the photocurrent density and the photoconductivity, have been  
24  
25 previously used to study the electrical response to light of different photogenerating materials  
26  
27 and devices.<sup>14-17</sup> Transient photocurrent experiments are also useful to obtain information about  
28  
29 trapping and recombination on time scales of up to 1  $\mu$ s after illumination.<sup>18</sup> In the present work  
30  
31 we use the steady-state photocurrent, since experiments are simple and precise, and results under  
32  
33 equilibrium conditions have the advantage of being widely applicable. Note that dark current is  
34  
35 subtracted from the current under illumination to determine a supposedly corrected photocurrent  
36  
37 that is independent of carrier injection at the electrodes.<sup>17</sup>

38  
39  
40  
41  
42  
43  
44  
45  
46 The work performed with PBI-W+LC is presented and discussed as follows: Firstly, the photo-  
47  
48 response at room temperature (RT = 22 °C) is studied as a function of the applied electric field,  
49  
50 in order to determine optimal conditions for subsequent measurements. Then, the photocurrent  
51  
52 dependence on temperature is analyzed, with the aim of obtaining, from changes in the activation  
53  
54 energy, singular temperatures delimiting different charge transport regimes. Finally, from  
55  
56  
57  
58  
59  
60

combined studies as a function of temperature and light intensity, charge recombination mechanisms are identified and their origin discussed.

## EXPERIMENTAL SECTION

The synthesis of PBI-W+LC was firstly reported by Hansen et al.<sup>19</sup> Here we made some small modifications to the procedure for the isolation and purification of the final product as previously described.<sup>9</sup> PBI-W+LC shows a LC phase between 60 and 111 °C and a crystalline-crystalline transition at 15 °C, as determined from DSC. Its structure is characteristic for discotic packing in which the PBI building blocks assemble into columns arranged in a hexagonal unit cell.<sup>9,19,20</sup>

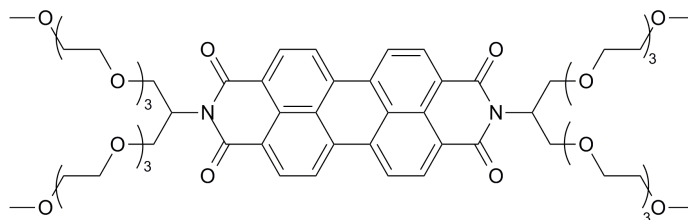


**Figure 1.-** Molecular structure of PBI-W+LC.

Samples for the photocurrent studies have been prepared by capillary-filling Linkam cells, consisting of two indium tin oxide (ITO)-coated parallel glass plates with a gap of 5.0  $\mu\text{m}$  and effective area 0.81  $\text{cm}^2$ , with the neat material in the isotropic phase (130 °C). The cells were then cooled down to room temperature at a rate of about 1 °C/min.<sup>9</sup> Conductivity measurements have been performed by a simple direct current (DC) technique using a picoammeter/voltage source HP 4140B to apply the voltage and to measure the current. A Melles-Griot He-Ne laser (633 nm) with a maximum light intensity of 25  $\text{mW}/\text{cm}^2$  was the light source selected to

1  
2  
3 illuminate the samples. Since absorption is low and the light distribution inside the material is  
4 quite uniform, the conductivity and photoconductivity values can be calculated without using  
5 correction factors.<sup>21</sup> Current densities in the absence of light,  $j_{\text{dark}}$ , and under illumination,  $j_{\text{light}}$ ,  
6 were measured. Then, the corrected photocurrent density,  $j_{\text{phot}}$ , defined as  $j_{\text{light}} - j_{\text{dark}}$ , was  
7 calculated. No further corrections were needed,<sup>22</sup> since as described in the section below, results  
8 correspond to the injection-limited current regime. Transients were registered with an  
9 oscilloscope to study the temporal evolution of currents. As a consequence, the value in each  
10 measurement was taken after the current reached a quasi-steady state ( $\approx 60$  s in the dark and  $\approx 10$   
11 s more after illuminating the sample). Presumably, the viscosity of the material in the liquid  
12 crystal phase is very high (the filling of the cell at 130 °C takes around 90 min). Besides, the  
13 material was highly purified.<sup>9</sup> So, even though neither viscosity nor impurities concentration  
14 were quantified, in our case ionic conduction processes, such as those observed in other liquid  
15 crystalline materials,<sup>23</sup> was not expected to contribute significantly to the conductivity. In the  
16 experiments for studying the temperature dependence of the photocurrent, samples were placed  
17 in a temperature-controlled set up regulated with an accuracy of  $\pm 0.5$  °C, and data were collected  
18 every 5 °C, while the temperature varied at a rate of 0.5 °C/min. Since each sample was used to  
19 make successive measurements of  $j_{\text{dark}}$  and  $j_{\text{phot}}$  from RT up to the transition temperature to the  
20 isotropic phase, it was important to work under moderate electric fields to prevent memory  
21 effects in the material.  
22  
23  
24  
25  
26  
27  
28  
29  
30  
31  
32  
33  
34  
35  
36  
37  
38  
39  
40  
41  
42  
43  
44  
45  
46  
47  
48  
49  
50  
51  
52  
53  
54  
55  
56  
57  
58  
59  
60

## RESULTS AND DISCUSSION

### **Dark current and photocurrent dependence on applied electric field**

The PDI-W+LC dark current and photocurrent, measured at RT and at a moderate light intensity ( $10 \text{ mW/cm}^2$ ), as a function of the strength and polarity of the applied electric-field are shown in Figure 2. Since the device is symmetric (ITO/PBI-W+LC/ITO), the dark current is independent of the bias polarity. On the other hand, the photocurrent is dependent of the bias polarity on the illuminated electrode, but only weakly, because of the relatively low absorption at 633 nm. Photocurrent increases rapidly, reaching values acceptably high ( $10^{-10}$ - $10^{-9} \text{ A/cm}^2$ ) to be measured with precision under fields lower than  $1 \text{ V}/\mu\text{m}$ . Thus, subsequent experiments as a function of temperature and light intensity were carried out under a negative bias (though this selection is not compulsory) of  $0.4 \text{ V}/\mu\text{m}$  and  $10 \text{ mW/cm}^2$ . According to the HOMO and LUMO values of PBI-W+LC,<sup>20</sup> the Shottky energy barrier of the device (see energy level diagram in the inset of Figure 2), is around 1 eV. Since this value is higher than 0.4 eV, which establishes the delimitation between regimes in which the current flow is space charge limited or injection limited,<sup>24</sup> it can be concluded than in our case the current is injection limited with a quite low injection efficiency. This means that currents are quite small, several orders of magnitude lower than those which would be obtained in a space-charge limited regime.



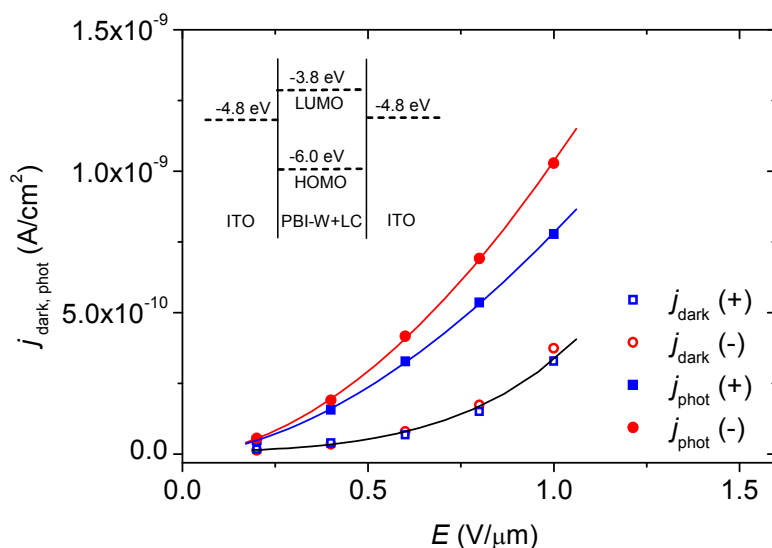


**Figure 2.-** Dark current,  $j_{\text{dark}}$ , and photocurrent,  $j_{\text{phot}}$ , densities for PBI-W+LC at room temperature (22°C) vs electric field,  $E$ , under positive and negative bias. The light intensity at 633 nm is 10 mW/cm<sup>2</sup>. Full lines are guides to the eye. The inset shows the energy level diagram of the device ITO/PBI-W+LC/ITO.

### Photocurrent dependence on temperature

The temperature dependence of dark current and photocurrent at a light intensity of 10 mW/cm<sup>2</sup> and at a negative bias of 0.4 V/μm are shown in Figure 3a. Since both,  $j_{\text{dark}}$  and  $j_{\text{phot}}$ , obey exponential laws of the form

$$j_{\text{dark,phot}} = j_{\text{dark0,phot0}} \exp\left(-\frac{\Delta E_{\text{dark,phot}}}{KT}\right) \quad (1)$$

where  $j_{\text{dark,phot}}$  is a pre-exponential factor,  $\Delta E_{\text{dark,phot}}$  is the activation energy and  $K$  is the Boltzmann constant, data are presented in Arrhenius diagrams (see Figure 3a). This expression is

1  
2  
3 used here empirically with the purpose of identifying with precision, from the changes in the  
4 photocurrent activation energy, the singular temperatures at which the photocurrent behavior  
5 changes. Note that understanding in depth the origin of the activation energy is not an obvious  
6 task, since it depends of many factors, such as the barriers between crystals, the amount and  
7 depth of traps, impurities, etc. It was established that from sample to sample the error in the  
8 currents is moderate, less than 10%. However the standard deviation in the transition  
9 temperatures is only  $\pm 1$  °C. For the whole temperature range explored, the photocurrent is higher  
10 than the dark current. Two appreciable changes can be observed at 60 °C, where the activation  
11 energy decreases from 0.82 eV to 0.68 eV; and at 110 °C, where the activation energy decreases  
12 again to 0.44 eV. These two temperatures coincide with those corresponding to the phase  
13 changes determined by DSC (see inset of Figure 3a), firstly from the crystalline (C) to the LC  
14 phase and then to the isotropic (I) phase. Highly remarkable is the observation of an abrupt  
15 change at 45 °C, where the activation energy increases from 0.14 eV to 0.82 eV, which it is not  
16 observed in the DSC thermogram and therefore cannot be related to a structural or phase change  
17 of the material. We note that the three singular temperatures observed by considering the  
18 photocurrent are not appreciated in the dark current line, for which the activation energy, 0.59  
19 eV, is constant in the whole range of temperatures explored. Also remarkable is the fact that the  
20 singular temperature observed at 45 °C could not be detected in our previous mobility study of  
21 PBI-W+LC,<sup>9</sup> probably because errors are higher than 10%, due to the dispersive character of the  
22 transport process (for clarity, these mobility data have been included in Figure 3a).

23  
24  
25  
26  
27  
28  
29  
30  
31  
32  
33  
34  
35  
36  
37  
38  
39  
40  
41  
42  
43  
44  
45  
46  
47  
48  
49  
50  
51 In Figure 3b it is shown that the use of the photosensitivity,  $S = j_{\text{phot}} / j_{\text{dark}}$ , as an alternative  
52 parameter to the photocurrent, allows improving the accuracy in determining these singular  
53 temperatures at which the dominating charge transport mechanism changes. Although other  
54  
55  
56  
57  
58  
59  
60

1  
2  
3 parameters such as the conductivity contrast,  $M = j_{\text{phot}} / j_{\text{light}}$ , could also be used for that purpose,  
4  
5  $S$  has the advantage respect to  $M$  that it stands out the relevant fact, as we show below, that the  
6  
7 kink at 45 °C takes place when dark current becomes of the order of the photocurrent ( $S \sim 1$ ). At  
8  
9 RT,  $S$  decreases with increasing temperature, while it remains relatively constant between the  
10  
11 temperatures that limit the LC phase. It can also be seen that the singular temperatures are very  
12  
13 well marked, especially the one at 45 °C. This suggests that the activation energy transition at 45  
14  
15 °C does not correspond to a pre-transitional change related to the phase transition observed in the  
16  
17 DSC thermogram at 60 °C, but to a change with a different origin.  
18  
19  
20  
21  
22  
23  
24  
25  
26  
27  
28  
29  
30  
31  
32  
33  
34  
35  
36  
37  
38  
39  
40  
41  
42  
43  
44  
45  
46  
47  
48  
49  
50  
51  
52  
53  
54  
55  
56  
57  
58  
59  
60

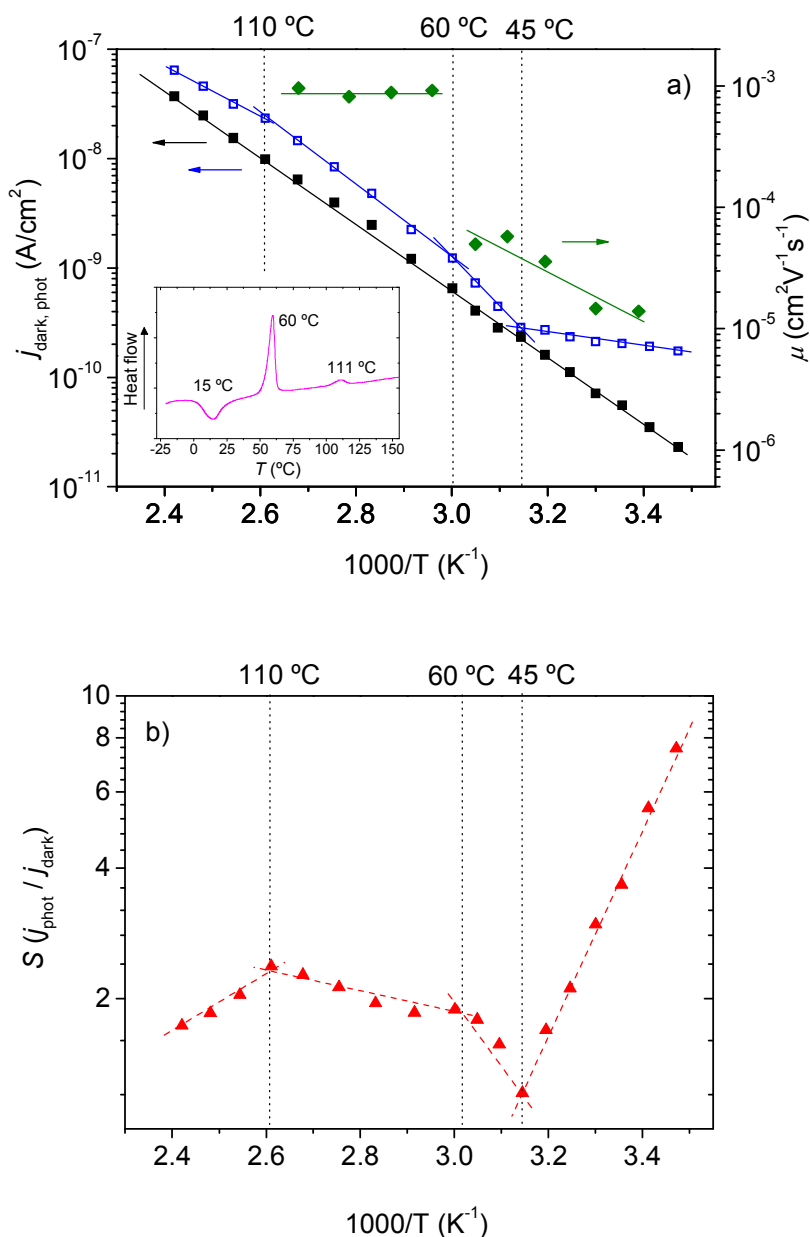


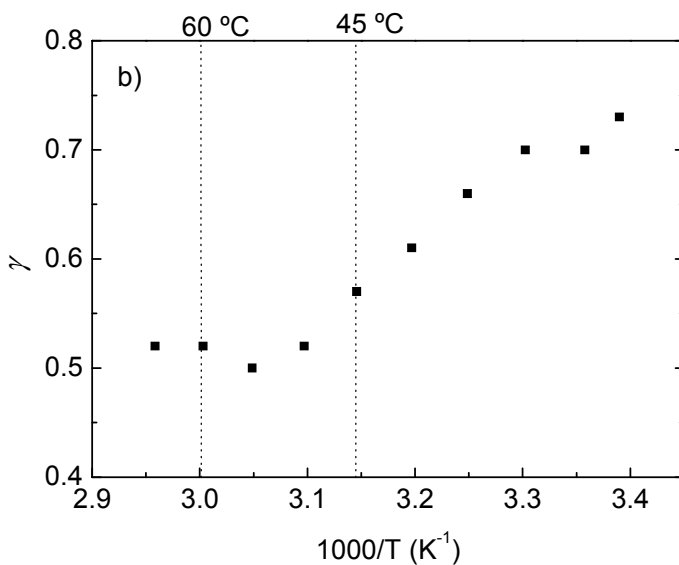
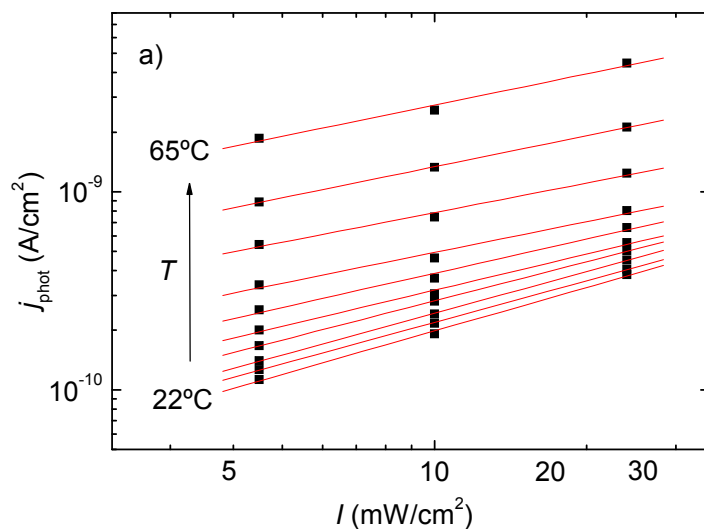
**Figure 3.-** Arrhenius plots of (a) dark current,  $j_{\text{dark}}$  (black full squares) and photocurrent  $j_{\text{phot}}$  (blue empty squares) and (b) photosensitivity  $S = j_{\text{phot}} / j_{\text{dark}}$  (red full triangles) at an electric field of  $0.4 \text{ V}/\mu\text{m}$ , and a light intensity of  $10 \text{ mW}/\text{cm}^2$  at  $633 \text{ nm}$  for PBI-W+LC. Solid lines are linear fits of experimental data to determine activation energies and dashed lines are guides to the eye. For comparison purposes, DSC (corresponding to the second heating cycle at a scanning rate of

1  
2  
3 10 K min<sup>-1</sup>) and mobility data for PBI-W+LC, taken from Ref. 9, are included in (a), inset and  
4  
5 green full diamonds plotted in right axis, respectively.  
6  
7

### 10 **Photocurrent dependence on light intensity at various temperatures**

11  
12 The observation of singular temperatures at which the conductivity activation energy changes  
13 has been reported in the literature for various p-type organic materials: Nitta et al.<sup>25</sup> in  
14 amorphous carbon nitride at  $\approx 400$  K; Ilie et al.<sup>14</sup> in different amorphous carbon derivatives at  $\approx$   
15 200 K; and Dulieu et al.<sup>15</sup> in polyparaphenylenevinylene (PPV) at  $\approx 160$  K. In this last case the  
16 activation energy change was assigned to a change from monomolecular to bimolecular  
17 recombination mechanism. This prompted us to investigate the light intensity dependence of the  
18 PBI-W+LC photocurrent at different temperatures (see Figure 4a) as to ascertain whether the  
19 change in the activation energy observed at 45 °C (318 K) corresponds to a change in the  
20 recombination mechanism, as it occurs in PPV. In organic materials, photocurrent follows a  
21 potential law,  $j_{\text{phot}} \propto I^\gamma$ , similar to that of the electric field dependence, where the exponent  $\gamma$ ,  
22 which can be obtained by fitting the experimental data to this power function, is related to the  
23 type of charge recombination mechanism. This parameter was used by other authors to identify  
24 the type of recombination mechanism in Phthalocyanine and C<sub>60</sub>.<sup>26,27</sup> They found  $\gamma$  values  
25 between 1 and 0.5, corresponding to monomolecular and bimolecular recombination,  
26 respectively. As shown in Figure 4a, the PBI-W+LC photocurrent dependence on light intensity  
27 at RT shows a sublinear behavior. By fitting the data to the function  $j_{\text{phot}} \propto I^\gamma$ , a  $\gamma$  value of 0.7  
28 was obtained. This means that part of electrons in the conduction band directly recombines with  
29 holes in the valence band, and other part recombines with holes through recombination centers in  
30 the gap. For higher temperatures,  $\gamma$  decreases with the increase of temperature, reaching a value  
31  
32  
33  
34  
35  
36  
37  
38  
39  
40  
41  
42  
43  
44  
45  
46  
47  
48  
49  
50  
51  
52  
53  
54  
55  
56  
57  
58  
59  
60

of 0.5 at temperatures higher than 45 °C (see Figure 4b). Consequently, at RT, where  $\gamma \approx 0.7$ , the mechanism is a mixture of monomolecular and bimolecular recombination, while above 45 °C it becomes a pure bimolecular mechanism. So in the range of temperatures explored, results coincide with those obtained with PPV at a lower temperature and under a similar applied electric field (0.2 V/ $\mu\text{m}$ ).



1  
2  
3 **Figure 4.-** (a) Log-log plot of the photocurrent density ( $j_{\text{phot}}$ ) for PBI-W+LC vs light intensity ( $I$ )  
4 at 633 nm at RT (bottom line) and at higher temperatures up to 65 °C (top line). Measurements  
5 were taken under negative electrode illumination, and the strength of the applied field was 1.0  
6 V/ $\mu\text{m}$ . The solid lines are fits to data with the function  $j_{\text{phot}} \propto I^\gamma$ , from which the parameter  $\gamma$  is  
7 determined; (b) Temperature dependence of  $\gamma$ .  
8  
9  
10  
11  
12  
13  
14  
15  
16  
17  
18

19 With regards to the cause of the recombination mechanism change, a possible explanation  
20 points to the influence of  $j_{\text{dark}}$  on  $j_{\text{phot}}$  when the temperature is increased. It can be observed in  
21 Figure 3 that the change in the activation energy in PBI-W+LC at 45 °C occurs when the  $j_{\text{dark}}$   
22 value becomes similar to  $j_{\text{phot}}$ , i.e. the total amount of charge carriers (not only the photocarriers  
23 computed to calculate  $j_{\text{phot}}$ ), increases appreciably. This fact can also be observed in the  
24 Arrhenius plots of other organic,<sup>14,25</sup> inorganic<sup>16,28</sup> and photorefractive<sup>10,11</sup> materials in which  
25  $j_{\text{dark}}$  and  $j_{\text{phot}}$  are presented simultaneously. For example, data in Figure 2 of Ref. 11 show the  
26 correlation between the transition temperatures and the abrupt increase of thermal carriers,  
27 although in that case the variable parameter is the frequency of the applied electric field. These  
28 activation energy changes can be interpreted by considering that the monomolecular  
29 recombination rate depends linearly with charge density and the bimolecular recombination rate  
30 is proportional to the square of the charge density.<sup>29</sup> In that case, in the presence of both  
31 mechanisms, bimolecular recombination will be more important at high charge density and  
32 monomolecular recombination will dominate at low charge density. The influence of the  
33 increased carrier density on the change from monomolecular to bimolecular recombination  
34 kinetics has been observed in polymer-fullerene bulk heterojunction solar cells where the charge  
35 density is very high.<sup>13</sup> In that case, the increase of the total number of carriers was due to a  
36  
37  
38  
39  
40  
41  
42  
43  
44  
45  
46  
47  
48  
49  
50  
51  
52  
53  
54  
55  
56  
57  
58  
59  
60

1  
2  
3 decrease of the applied field, i.e. a decrease of the carrier sweep-out. It is also important to stress  
4 that according to the photocurrent definition,  $j_{\text{phot}} = j_{\text{light}} - j_{\text{dark}}$ , it seems that the effect of thermal  
5 carriers is subtracted. However, this is only true when the thermal carrier density is quite smaller  
6 than that of the photocarriers. When the amount of both densities becomes of the same  
7 magnitude, thermal carriers affect the recombination mechanism and, consequently, the  
8 photocarriers transport.  
9

10  
11 In order to explore how sensitive the transition temperature observed at 45°C is to changes on  
12 the light intensity, we have performed additional temperature-dependent photocurrent  
13 experiments in the crystalline phase at light intensities of 4.5 and 20 mW/cm<sup>2</sup>. These data,  
14 together with those obtained at 10 mW/cm<sup>2</sup>, already included in Figure 3, are shown in  
15 Arrhenius-type plots in Figure 5. Results show that both, the transition temperature and the  
16 sensitivity  $S$ , increase with the illumination level from 43 °C to 48 °C, and from about 1 to 2,  
17 respectively. According to these results, the activation energy transition corresponds to a value of  
18  $S$  of around 1, more specifically, to a value  $S < 1$  for low light levels and  $S > 1$  for high light  
19 levels. Remarkably, the activation energy values, below and above the transition temperature, are  
20 independent of light intensity, and the only change produced by the change in the total density of  
21 carriers (due to a change of illumination level) is the shift of the transition temperature at which  
22 the recombination mechanism changes. Such shifts of the transition temperature when the light  
23 intensity level varies, have also been observed by other authors in other types of materials.<sup>25</sup>  
24  
25  
26  
27  
28  
29  
30  
31  
32  
33  
34  
35  
36  
37  
38  
39  
40  
41  
42  
43  
44  
45  
46  
47  
48  
49  
50  
51  
52  
53  
54  
55  
56  
57  
58  
59  
60



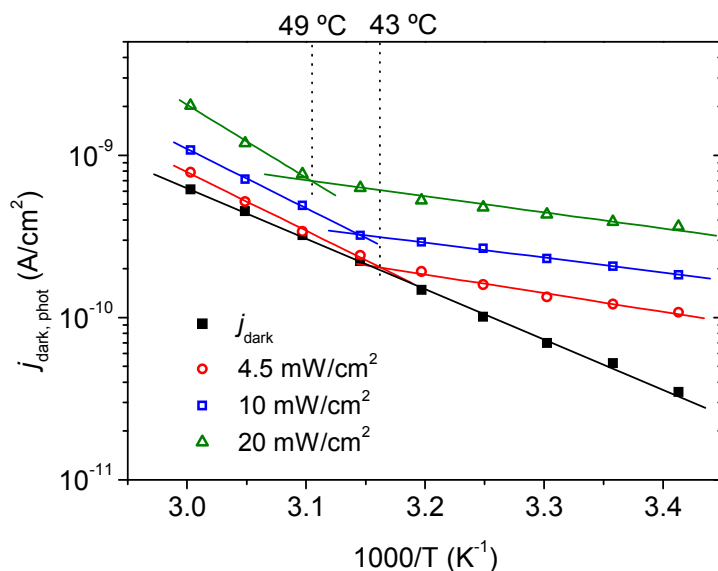


**Figure 5.** Arrhenius plots of dark current,  $j_{\text{dark}}$  (black full squares), and photocurrent  $j_{\text{phot}}$  for  $4.5 \text{ mW}/\text{cm}^2$  (red empty circles),  $10 \text{ mW}/\text{cm}^2$  (blue empty squares) and  $20 \text{ mW}/\text{cm}^2$  (green empty triangles) at an electric field of  $0.4 \text{ V}/\mu\text{m}$  in PBI-W+CL.

The applicability of the methodology proposed in this work to other materials was studied by performing some photocurrent experiments with films of the PBI compound N,N'-Bis(1-hexylheptyl)-perylene-3,4:9,10-bis-(dicarboximide) (PBI-C6, chemical structure in Figure S1, Supporting Information) which is neither water soluble, nor LC. This material is crystalline in the whole temperature range from RT to the isotropic phase, so no phase transition temperatures are observed in its DSC diagram, except for the obvious C-I one, at  $144^\circ\text{C}$ .<sup>9</sup> Also in this case singular temperatures were observed in the Arrhenius plots of the photocurrent and the photosensitivity, particularly at  $50$  and  $85^\circ\text{C}$  (see Figure S2 in Supporting Information), which do not appear in the DSC thermogram. Unfortunately, a photocurrent study of PBI-C6 as a function of light intensity, such as the one performed with PB-W+LC, to get insights into the

1  
2  
3 origin of these transitions, could not be performed since the photosensitivity of this material is  
4 rather low (see SI for additional discussions). Despite the difficulties in some cases, such as in  
5 PDI-C6, of providing a precise explanation of the underlying transport mechanisms causing  
6 these singular temperatures, which are not connected with structural or phase transitions, but  
7 with the fact that thermal carriers get of the same order of magnitude than that of the  
8 photocarriers, the key point is that they appear in a wide variety of semiconducting  
9 photogenerating materials,<sup>14-16,25,28</sup> not necessarily PBIs, or even organic semiconductors. This  
10 suggests that the methodology proposed here might possibly be applied to study other materials,  
11 whenever they are both, charge transporters and photogenerators. Nevertheless, further studies to  
12 clarify aspects such as the origin of the dark current and the photocurrent, or the influence of  
13 working in charge injection regime, are still needed to reach such ambitious goal.  
14  
15  
16  
17  
18  
19  
20  
21  
22  
23  
24  
25  
26  
27  
28  
29  
30  
31

## 32 CONCLUSIONS

33  
34 In summary, temperature-dependent steady-state photocurrent measurements have been  
35 performed in PBI-W+LC. Through the observed changes in the activation energy, the structural  
36 or phase transition temperatures and other singular temperatures at which variations in the  
37 transport mechanisms occur, have been determined with accuracy. Transport behavior changes  
38 were observed at 60 °C and 110 °C, related to phase changes from crystalline to LC and from LC  
39 to isotropic phases, respectively, as confirmed by DSC. In addition, a transition at 45 °C has been  
40 observed, which cannot be detected by either DSC, or by mobility data. From the analysis of the  
41 light intensity dependent photocurrent at different temperatures, this singular temperature is  
42 interpreted as a change from monomolecular to bimolecular recombination, which occurs when  
43 the thermal carrier density becomes of the same magnitude than that of the photocarriers. The  
44  
45  
46  
47  
48  
49  
50  
51  
52  
53  
54  
55  
56  
57  
58  
59  
60

1  
2  
3 fact that singular temperatures connected with this phenomenon haven been reported in the  
4 literature for other kind of semiconducting photogenerating materials, suggests that the proposed  
5 analysis methodology might be useful for other systems.  
6  
7  
8  
9

## 10 11 12 AUTHOR INFORMATION

### 13 14 **Corresponding Author**

15  
16  
17 \* Corresponding author. Phone: +34 96 590 3543; Fax +34 96 590 9726. Email:  
18 maria.diaz@ua.es  
19  
20  
21  
22

## 23 24 ACKNOWLEDGMENT

25  
26  
27  
28 We thank support from the Spanish Government (MINECO) and the European Community  
29 (FEDER) through grant MAT-2011-28167-C02-01, as well as to the University of Alicante. We  
30 also acknowledge Dr. P.G. Boj for useful discussions and V. Esteve for technical assistance.  
31  
32 Financial support from MINECO (CTQ2010-14982) and Comunidad Autónoma de Madrid  
33 (S2009/MAT-1467) is gratefully acknowledged. A. de la Peña thanks Universidad Complutense  
34 for a predoctoral fellowship.  
35  
36  
37  
38  
39  
40  
41  
42

## 43 44 ASSOCIATED CONTENT

### 45 46 Supporting Information Available

47  
48  
49 Additional Supporting Information about the molecular structure, and Arrhenius plots of dark  
50 current, photocurrent and phosensitivity of PBI-C6. The Supporting Information is available free  
51 of charge via the Internet at <http://pubs.acs.org>  
52  
53  
54  
55  
56  
57  
58  
59  
60

## REFERENCES

- 1 Zhan, X.; Facchetti, A.; Barlow, S.; Marks, T. J.; Ratner, M. A.; Wasielewski, M. R.; Marder, S. R. Rylene and Related Diimides for Organic Electronics. *Adv. Mater.* **2011**, *2*, 268-284.
- 2 Li, C.; Wonneberger, H. Perylene Imides for Organic Photovoltaics: Yesterday, Today, and Tomorrow. *Adv. Mater.* **2012**, *24*, 613-636.
- 3 Kim, Y.; Chung, I.; Kim, Y. C.; Yu, J. Mobility of Electrons and Holes in a Liquid Crystalline Perylene Diimide Thin Film with Time of Flight Technique. *Chem. Phys. Lett.* **2004**, *398*, 367-371.
- 4 Duzhko, V.; Aqad, E.; Imam, M. R.; Peterca, M.; Percec, V.; Singer, K. D. Long-Range Electron Transport in a Self-Organizing n-Type Organic Material. *Appl. Phys. Lett.* **2008**, *113*, 113312.
- 5 Muth, M. A.; Gupta, G.; Wicklein, A.; Carrasco-Orozco, M.; Thurn-Albrecht, T.; Thelakkat, M. Crystalline vs Liquid Crystalline Perylene Bisimides: Improved Electron Mobility Via Substituent Alteration. *J. Phys. Chem. C* **2014**, *118*, 92-102.
- 6 Backes, C.; Schmidt, C. D.; Rosenlehner, K.; Hauke, F.; Coleman, J. N.; Hirsch, A. Nanotube Surfactant Design: The Versatility of Water-Soluble Perylene Bisimides. *Adv. Mater.* **2010**, *22*, 788-802.
- 7 Görl, D.; Zhang, X.; Würthner, F. Molecular Assemblies of Perylene Bisimide Dyes in Water. *Angew. Chem. Int. Ed.* **2012**, *51*, 6328-6348.

1  
2  
3 8 Heek, T.; Nikolaus, J.; Schwarzer, R.; Fasting, C.; Welker, P.; Licha, K.; Herrmann, A.;  
4 Haag, R. An Amphiphilic Perylene Imido Diester for Selective Cellular Imaging. *Bioconjugate*  
5  
6 *Chem.* **2013**, *24*, 153-158.  
7

8  
9  
10  
11 9 Quintana, J. A.; Villalvilla, J. M.; de la Peña, A.; Segura, J. L.; Díaz-García, M. A.  
12  
13 Electron Transport in a Water-Soluble Liquid-Crystalline Perylene Bisimide. *J. Phys. Chem. C*  
14  
15 **2014**, *118*, 26577-26583.  
16

17  
18  
19 10 Quintana, J. A.; Boj, P. G.; Villalvilla, J. M.; Díaz-García, M. A.; Ortiz, J.; Martín-  
20  
21 Gomis, L.; Fernández-Lázaro, F.; Sastre-Santos, A. Determination of the Glass Transition  
22  
23 Temperature of Photorefractive Polymer Composites from Photoconductivity Measurements.  
24  
25 *Appl. Phys. Lett.* **2008**, *92*, 041101.  
26  
27

28  
29  
30 11 Villalvilla, J. M.; Díaz-García, M. A.; Quintana, J. A.; Boj, P. G. Critical Temperatures in  
31  
32 the Photorefractive Polymer Composite Behavior. *J. Phys. Chem. Lett.* **2010**, *1*, 383-387.  
33

34  
35 12 Riedel, I.; Parisi, J.; Dyakonov, V.; Lutsen, L.; Vanderzande, D.; Hummelen, J. C. Effect  
36  
37 of Temperature and Illumination on the Electrical Characteristics of Polymer-Fullerene Bulk-  
38  
39 Heterojunction Solar Cells. *Adv. Func. Mater.* **2004**, *14*, 38-44.  
40

41  
42  
43 13 Cowan, S. R.; Roy, A.; Heeger, A. J. Recombination in Polymer-Fullerene Bulk  
44  
45 Heterojunction Solar Cells. *Phys. Rev. B*, **2010**, *82*, 245207.  
46  
47

48  
49 14 Ilie, A.; Conway, N. M. J.; Kleinsorge, B.; Robertson, J.; Milne, W. I. Photoconductivity  
50  
51 and Electronic Transport in Tetrahedral Amorphous Carbon and Hydrogenated Tetrahedral  
52  
53 Amorphous Carbon. *J. Appl. Phys.* **1998**, *84*, 5575-5582.  
54  
55

1  
2  
3 15 Dulieu, B.; Wéry, J.; Lefrant, S.; Bullo, J. Intrinsic and Extrinsic Photocarriers in  
4 Polyparaphenylenevinylene. *Phys. Rev. B* **1998**, *57*, 9118-9127.  
5  
6

7  
8  
9 16 Esmaeili-Rad, M. R.; Sazonov, A.; Kazanskii, A. G.; Khomich, A. A.; Nathan, A.  
10 Optical Properties of Nanocrystalline Silicon Deposited by PECVD. *J. Mater. Sci: Mater.*  
11 *Electron* **2007**, *18*, S405-S409.  
12  
13  
14

15  
16  
17 17 Oui, Z. E.; Jin, R.; Huang, J.; Loo, Y. F.; Sellinger, A.; deMello, J. C. On the Pseudo-  
18 Symmetric Current-Voltage Response of Bulk Heterojunction Solar Cells. *J. Mater. Chem.* **2008**,  
19 *18*, 1644-1651.  
20  
21  
22

23  
24  
25 18 Day, J.; Subramanian, S.; Anthony, J. E.; Lu, Z.; Twieg, R. J.; Ostroverkhova, O.  
26 Photoconductivity in Organic Thin Films: From Picoseconds to Seconds after Excitation. *J.*  
27 *Appl. Phys.* **2008**, *103*, 123715.  
28  
29  
30

31  
32  
33 19 Hansen, M. R.; Schnitzler, T.; Pisula, W.; Graf, R.; Müllen, K.; Spiess, H. W.  
34 Cooperative Molecular Motion within a Self-Assembled Liquid-Crystalline Molecular Wire: The  
35 Case of a TEG-Substituted Perylenediimide Disc. *Angew. Chem. Int. Ed.* **2009**, *48*, 4621-4624.  
36  
37  
38

39  
40  
41 20 Wicklein, A.; Lang, A.; Muth, M.; Thelakkat, M. Swallow-Tail Substituted Liquid  
42 Crystalline Perylene Bisimides: Synthesis and Thermotropic Properties. *J. Am. Chem. Soc.* **2009**,  
43 *131*, 14442-14453.  
44  
45  
46

47  
48  
49 21 Ostroverkhova, O.; Moerner, W. E. High-Performance Photorefractive Organic Glass  
50 with Near-Infrared Sensitivity. *Appl. Phys. Lett.* **2003**, *82*, 3602-3604.  
51  
52  
53  
54  
55  
56  
57  
58  
59  
60

1  
2  
3 22 Wehenkel, D. J.; Koster, L. J. A.; Wienk, M. M.; René A. J. Janssen, R. A. J. Influence of  
4  
5 Injected Charge Carriers on Photocurrents in Polymer Solar Cells. *Phys. Rev. B* **2012**, 85,  
6  
7 125203-1-125203-12.  
8  
9

10  
11 23 Ahn, H; Ohno, A.; Hanna, J. Impurity Effects on Charge Carrier Transport in Various  
12  
13 Mesophases of Smectic Liquid Crystals. *J. Appl. Phys.* **2008**, 102, 093718-1-093718-6.  
14  
15

16  
17 24 Campbell, H; Davids, P.S.; Smith, D.L.; Barashkov, N. N.; Ferraris, J. P. The Schottky  
18  
19 Energy Barrier Dependence of Charge Injection in Organic Light-Emitting Diodes. *Appl. Phys.*  
20  
21 *Lett.* **1998**, 72, 1863-1865.  
22  
23

24  
25 25 Nitta, S.; Takada, N.; Sugiyama, K.; Itoh, T.; Nonomura, S. Preparation and Properties of  
26  
27 Photoconductive Amorphous Carbon Nitride a-CN<sub>x</sub> Films: The Layer-by-Layer Method. *J. Non-*  
28  
29 *Cryst. Solids* **1998**, 227–230, 655–658.  
30  
31

32  
33 26 Heilmeyer, G. H.; Harrison, S. E. Implications of the Intensity Dependence of  
34  
35 Photoconductivity in Metal-Free Phthalocyanine Crystals. *J. Appl. Phys.* **1963**, 34, 2732-2735.  
36  
37

38  
39 27 Hamed, A.; Escalante, R.; Hor, P. H.. Light-Intensity Dependence of the  
40  
41 Photoconductivity in C<sub>60</sub> Films. *Phys. Rev. B*, **1994**, 50, 8050-8053.  
42  
43

44  
45 28 Karaagac, H.; Parlak, M. The Investigation of Structural, Electrical, and Optical  
46  
47 Properties of Thermal Evaporated AgGaS<sub>2</sub> Thin Films. *Thin Solid Films* **2011**, 519, 2055-2061.  
48  
49

50  
51 29 Kao, K. C. *Dielectric Phenomena in Solids: With Emphasis on Physical Concepts of*  
52  
53 *Electronic Processes*; Elsevier Academic Press: San Diego, 2004.  
54  
55  
56  
57  
58  
59  
60

1  
2  
3 For Table of Contents Only  
4  
5  
6  
7  
8  
9

